

Cite this: *Chem. Sci.*, 2012, **3**, 2282

www.rsc.org/chemicalscience

EDGE ARTICLE

# Pb(II) metal–organic nanotubes based on cyclodextrins: biphasic synthesis, structures and properties†

Yanhui Wei,<sup>a</sup> Di Sun,<sup>a</sup> Daqiang Yuan,<sup>b</sup> Yongjun Liu,<sup>a</sup> Yi Zhao,<sup>a</sup> Xiyu Li,<sup>a</sup> Suna Wang,<sup>c</sup> Jianmin Dou,<sup>c</sup> Xingpo Wang,<sup>a</sup> Aiyu Hao<sup>a</sup> and Daofeng Sun<sup>\*ab</sup>

Received 14th February 2012, Accepted 18th April 2012

DOI: 10.1039/c2sc20187a

Two chiral lead metal–organic nanotubes (**CD-MONT-2** and **CD-MONT-3**) based on  $\beta$ -cyclodextrin ( $\beta$ -CD) and  $\gamma$ -cyclodextrin ( $\gamma$ -CD) were synthesized through a biphasic solvothermal reaction. The lead ions were connected by two  $\beta$ -CD or  $\gamma$ -CD molecules through their glycosidic oxygen atoms to generate a discrete metal–organic nanotube containing a  $\{\text{Pb}_{14}\}$  or  $\{\text{Pb}_{16}\}$  metallamacrocycle, respectively. Guest solvents of cyclohexanol molecules were trapped in the cavity of the  $\beta$ -CD-based nanotube, whereas there were no solvents in the cavity of the  $\gamma$ -CD-based nanotube. These differences directly led to the formation of different 3D packing structures. Their properties including temperature-dependent photoluminescence, adsorption of  $\text{I}_2$  molecules and thermal-decomposition behaviors were studied.

## Introduction

Metal–organic nanotubes (MONTs) or nanotubular architectures, as a special type of porous materials, have been attracting considerable attention from chemists and material scientists, due to their potential applications in the areas of gas adsorption, fluorescence and molecular sieves.<sup>1,2</sup> For assembly of MONTs, it seems especially important to carefully choose organic ligands and metal ions, search crystallization conditions, including even the inclusion of guest molecules, and adopt appropriate synthesis strategies. Thanks to the development of supramolecular chemistry and crystal engineering, the application of multifunctional organic ligands to connect metal ions has led to numerous finite or infinite MONTs or nanotubular architectures.<sup>3,4</sup> In particular, discrete MONTs remain less common to date.<sup>5</sup> Recently, we and other groups successfully assembled 1D non-interpenetrating MONTs based on mixed organic ligands under conventional or hydro/solvothermal conditions.<sup>6</sup> Herein, we report two chiral discrete MONTs based on cyclodextrin (CD) synthesized through the biphasic scenario.

As is well-known, CDs are water-soluble and biocompatible compounds, which makes them good candidates for functional

supramolecular assemblies and use in sophisticated drug delivery systems.<sup>7</sup> From a design perspective, CDs have a large number of glycosidic oxygen atoms and can provide plenty of coordination sites to chelate metal ions. Most reported complexes with CDs are aggregates formed by host–guest complexation.<sup>8</sup> Surprisingly, metal–organic complexes based on CDs remain less explored because of the difficulty in crystallization when coordinated to metal ions.<sup>9</sup> However, by adopting an appropriate synthetic strategy, it is possible to construct CD-based metal–organic complexes.

Very recently, Stoddart and coworkers reported a 3D porous framework based on  $\gamma$ -CD by a diffusion method.<sup>10</sup> Although Klufers *et al.* reported a Pb complex based on  $\gamma$ -CD molecule,<sup>11</sup> there is no systematic research on its properties and the effect of guest solvents on the 3D packing of metal complexes. In this work, we describe the synthesis and properties of discrete MONTs (**CD-MONT-2** and **CD-MONT-3**) based on  $\beta$ -CD and  $\gamma$ -CD (Scheme 1). We believe that our success in assembling **CD-MONT-2** and **CD-MONT-3** derives from the use of biphasic solvothermal synthesis, which has found an important niche in the preparation of inorganic–organic hybrid materials and coordination polymers.<sup>12</sup> High yield and purity of **CD-MONT-2** and **CD-MONT-3** were readily obtained through a biphasic solvothermal reaction of  $\text{PbCl}_2$  and  $\beta$ -CD or  $\gamma$ -CD in water and cyclohexanol. **CD-MONT-2** is slightly soluble in DMSO, however, **CD-MONT-3** is insoluble in common organic solvents.

## Experimental section

### Materials and methods

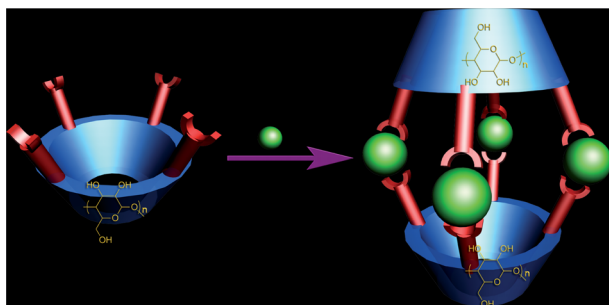
Commercially available reagents were used as received without further purification. Both cyclodextrins were further purified by recrystallization from water. <sup>1</sup>H NMR spectra were recorded on

<sup>a</sup>Key Lab for Colloid and Interface Chemistry of Education Ministry, School of chemistry and Chemical Engineering, Shandong University, Jinan 250100, People's Republic of China. E-mail: dfsun@sdu.edu.cn; Fax: +86-531-88364218

<sup>b</sup>State Key Laboratory of Structural Chemistry, Fujian Institute of Research on the Structure of Matter, Chinese Academy of Sciences, Fujian, Fuzhou, 350002, People's Republic of China

<sup>c</sup>Department of Chemistry, Liaocheng University, Liaocheng, 252059, People's Republic of China

† Electronic supplementary information (ESI) available. CCDC reference numbers: 859135 for **CD-MONT-2**, 859136 for **CD-MONT-3**. For ESI and crystallographic data in CIF or other electronic format see DOI: 10.1039/c2sc20187a



**Scheme 1** A schematic representation of CD molecules chelating metal ions to form MONT. For clarity, only four chelating groups are shown in each CD molecule.

a Bruker AVANCE-400 NMR Spectrometer. Elemental analysis was carried out on a CE instruments EA 1110 elemental analyzer. Photoluminescence spectra were performed on a F-280 Fluorescence Spectrophotometer. X-ray powder diffractions were measured on a Bruker AXS D8 Advance. Thermogravimetric analysis (TGA) was carried out in a static  $N_2$  with a heating rate of  $10\text{ }^\circ\text{C min}^{-1}$ . CD spectra were recorded on a JASCO J-810. SEM was obtained on a JEOL JSM-6700F. The UV-Vis absorption spectra were performed on a 2800UV/VIS Spectrophotometer.

### Synthesis of CD-MONT-2 and CD-MONT-3

**Synthesis of CD-MONT-2.**  $\beta$ -CD (0.02 mmol, 23 mg) and  $PbCl_2$  (0.16 mmol, 45 mg) were suspended in distilled water (6 mL). The mixture was stirred at  $80\text{ }^\circ\text{C}$  until precipitate stopped forming. After the removal of precipitate, the mixture was transformed to a glass tube, then mixed solvent (6 mL) of cyclohexanol and triethylamine ( $v/v = 1 : 1$ ) was slowly added. The glass tube was sealed and heated at  $110\text{ }^\circ\text{C}$  for 3 days (heating rate:  $16\text{ }^\circ\text{C h}^{-1}$ ; cooling rate:  $6\text{ }^\circ\text{C h}^{-1}$ ). A lot of colourless crystals were collected by filtration, washed with distilled water and dried in air (yield: 80%). Elemental analysis calcd (%) for **CD-MONT-2**: C 20.08, H 4.06; found: C 20.08, H 4.21%. Based on the EA, the formula of **CD-MONT-2** should be  $[Pb_{14}(\beta\text{-CD})_2] \cdot 3C_6H_{12}O \cdot 35H_2O$ .

**Synthesis of CD-MONT-3.** Reactions using  $\gamma$ -CD (0.02 mmol, 26 mg) and  $PbCl_2$  (0.018 mmol, 50 mg) were carried out as described above. The method of synthesis is similar to that of **CD-MONT-2** excepted that the proportion of mixed solvent of cyclohexanol and triethylamine is changed to  $1 : 4$  ( $v/v$ ). Yield: 70%. Elemental analysis calcd (%) for **CD-MONT-3**: C 18.66, H 3.07; found: C 18.65, H 3.12%. Based on the EA, the formula of **CD-MONT-3** should be  $[Pb_{16}(\gamma\text{-CD})_2] \cdot 14H_2O$ .

### X-ray crystallography

Single crystals of the **CD-MONT-2** and **CD-MONT-3** with appropriate dimensions were chosen under an optical microscope and mounted on a glass fiber for data collection. Single-crystal X-ray diffraction was performed using a Bruker Apex II CCD diffractometer equipped with a fine-focus sealed-tube X-ray source (Mo- $K\alpha$  radiation, graphite monochromated).

A preliminary orientation matrix and unit cell parameters were determined from 3 runs of 12 frames each, each frame corresponds to a  $0.5^\circ$  scan in 5 s, followed by spot integration and least-squares refinement. Data were measured using  $\omega$  scans of  $0.5^\circ$  per frame for 20 s until a complete hemisphere had been collected. Cell parameters were retrieved using SMART software and refined with SAINT on all observed reflections.<sup>13</sup> Data reduction was performed with the SAINT software and corrected for Lorentz and polarization effects. Absorption corrections were applied with the program SADABS.<sup>13</sup> In both cases, the highest possible space group was chosen. Both structures were solved by direct methods using SHELXS-97<sup>14a</sup> and refined on  $F^2$  by full-matrix least-squares procedures with SHELXL-97.<sup>14b</sup> Atoms were located from iterative examination of difference  $F$ -maps following least squares refinements of the earlier models. Hydrogen atoms were placed in calculated positions with isotropic displacement parameters set to  $1.2 \times U_{eq}$  of the attached atom.

## Results and discussion

### Structure analysis of CD-MONT-2 and CD-MONT-3

Single-crystal X-ray diffraction reveals that **CD-MONT-2** and **CD-MONT-3** crystallize in chiral orthorhombic  $P2_12_12_1$  space group and monoclinic  $P2_1$  space group with the Flack factors being  $-0.007(4)$  and  $0.041(9)$ , respectively. All of the glycosidic OH groups of  $\beta$ -CD and  $\gamma$ -CD are deprotonated during the biphasic solvothermal reaction and each one adopts a bidentate bridging mode to link two lead ions. Thus, 14 or 16 lead ions were chelated by 28 or 32 glycosidic oxygen atoms of two  $\beta$ -CD or  $\gamma$ -CD molecules to form the large  $\{Pb_{14}\}$  or  $\{Pb_{16}\}$  metallamacrocycles (Fig. 1), in which each lead ion is coordinated by four glycosidic oxygen atoms from two  $\beta$ -CD or  $\gamma$ -CD molecules. The average  $Pb \cdots Pb$  distances in the  $\{Pb_{14}\}$  and  $\{Pb_{16}\}$  metallamacrocycles are 3.832 and 3.830 Å, respectively. Due to the inherent symmetry of  $\beta$ -CD and  $\gamma$ -CD, there is a *pseudo*-seven-fold rotation axis in the  $\{Pb_{14}\}$  metallamacrocycle with rotation angles from  $50.07^\circ$  to  $52.18^\circ$  (the ideal rotation angle for the  $C_7$  axis is  $51.43^\circ$ ). While a *pseudo*- $C_8$  axis exists in the  $\{Pb_{16}\}$  metallamacrocycle (Fig. 1(f)), the rotation angles fall in the range  $43.54\text{--}46.06^\circ$  (the ideal rotation angle for the  $C_8$  axis is  $45^\circ$ ). As we know, molecules with a seven or eight-fold rotation axis are rare amongst reported structures.<sup>15</sup>

In the last few decades, many metallamacrocycles based on transition metal ions, lanthanide ions, or combinations of both have been successfully designed and synthesized. However, most reports are limited to low-nuclearity metallamacrocycles, such as  $\{M_2\}$ ,  $\{M_4\}$ ,  $\{M_6\}$  and  $\{M_8\}$  metallamacrocycles,<sup>16</sup> including a calixarene-based six-nuclearity lead example.<sup>17</sup> Up to now, only  $\{M_{10}\}$ ,  $\{M_{12}\}$ ,  $\{M_{15}\}$ ,  $\{M_{16}\}$ ,  $\{M_{20}\}$  and  $\{M_{24}\}$  high-nuclearity metallamacrocycles have been documented.<sup>18</sup> Chiral high-nuclearity metallamacrocycles are still less common. To date and to the best of our knowledge, only one example of a chiral high-nuclearity metallamacrocycle,  $[Mn_{15}L_{15}S_{15}]$  ( $L = N$ -phenyl-propionylsalicylhydrazide;  $S =$  solvents), has been reported.<sup>19</sup> Reports of high-nuclearity chiral metallamacrocycles, such as **CD-MONT-2** and **CD-MONT-3**, remain rare in the literature. The dimensions of the chiral cavity are about  $13.0 \times 10.3 \times 10.2\text{ \AA}$

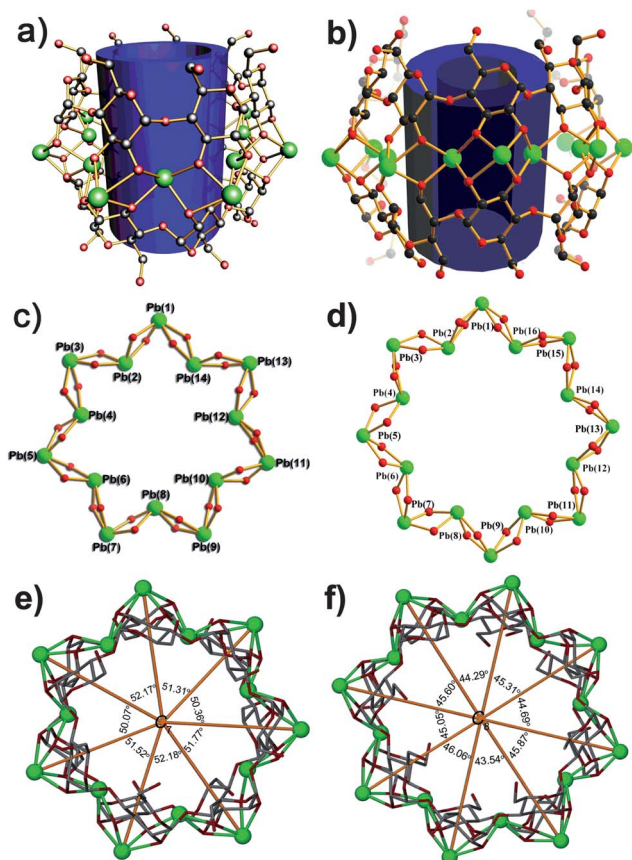


**Fig. 1** (a) and (b) the MONTs of **CD-MONT-2** and **CD-MONT-3**, respectively; (c) the fourteen-nuclearity lead metallamacrocycle in **CD-MONT-2**; (d) the sixteen-nuclearity lead metallamacrocycle in **CD-MONT-3**; (e) and (f) illustrations showing the *pseudo*- $C_7$  axis and *pseudo*- $C_8$  axis in the  $\{Pb_{14}\}$  and  $\{Pb_{16}\}$  metallamacrocycles, respectively.

and  $13.0 \times 12.9 \times 12.0$  Å for **CD-MONT-2** and **CD-MONT-3**, respectively. Although **CD-MONT-3** possesses a larger cavity than **CD-MONT-2**, there is no solvent guest such as cyclohexanol molecules in the chiral cavity of **CD-MONT-3** (Fig. S1†), which is quite different from a previous report by Klufers *et al.*<sup>11</sup> However, three cyclohexanol molecules were trapped in the chiral cavity of **CD-MONT-2**, two of which are located up and down the  $\{Pb_{14}\}$  ring and one occupies the window of the nanotube. The reason why there are no cyclohexanol molecules in the chiral cavity of **CD-MONT-3** may be that **CD-MONT-3** possesses a larger cavity, which results in the van der Waals interactions between the cyclohexanol molecules and the host is very weak.

It has been reported that the guest solvents in the cavity of CD molecules have a significant effect on the arrangement/packing of the host molecules.<sup>20</sup> Thus, due to the existence of cyclohexanol guest solvents and van der Waals interactions between the guests and the CD cavity, all of the **CD-MONT-2** molecules extend along the [100] direction, resulting in the formation of an infinite supramolecular MONT (Fig. 2(a, b)). The 3D packing of the molecules generates 1D channels along the *a* axis (Fig. 2(c)). A large amount of uncoordinated water molecules reside among the supramolecular MONTs. The solvent-accessible volume after the removal of uncoordinated solvents is 29.8%, which is calculated from the software PLATON.<sup>21</sup> However, there are two

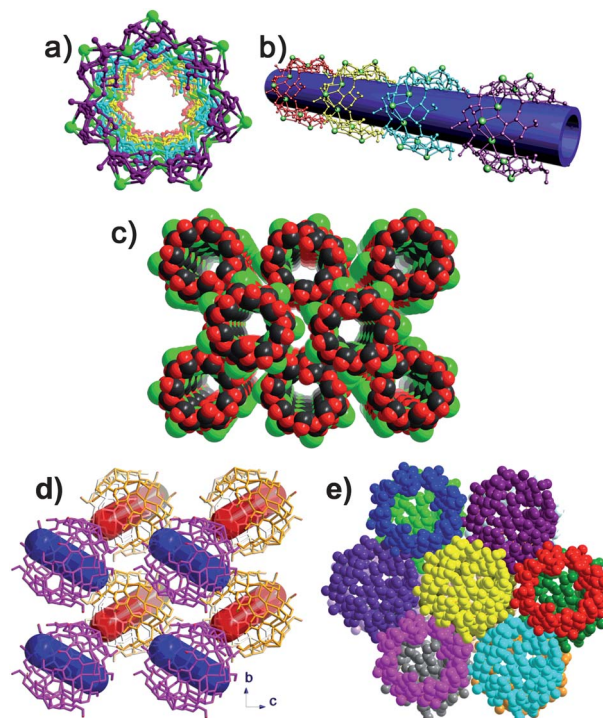


**Fig. 2** (a) and (b) the 1D supramolecular MONT of **CD-MONT-2** along different directions; (c) a space-filling representation of the 3D packing of **CD-MONT-2** showing the 1D channels; (d) the arrangement of **CD-MONT-3** along two different directions; (e) the 3D packing of **CD-MONT-3**.

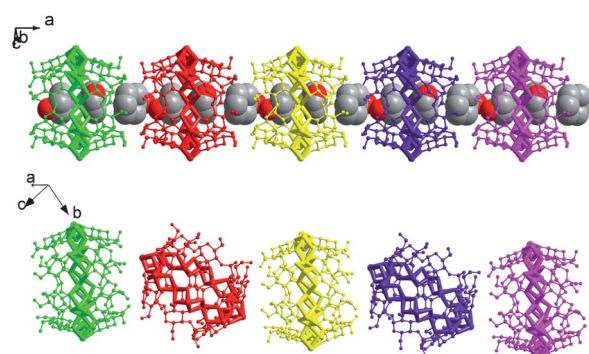


**Fig. 3** The different arrangement of **CD-MONT-2** (top) and **CD-MONT-3** (bottom) along one direction under the effect of guest solvents. The guests in **CD-MONT-2** are shown in a space-filling mode.

different packing directions in **CD-MONT-3**: one is along the [111] direction and the other is along the  $[1\bar{1}1]$  direction (Fig. 2(d)). The different packing directions block the channels from each other, resulting in a nonporous supramolecular architecture (Fig. 2(e)). These results further indicate that the guests have a significant effect on the packing of not only CD molecules but also CD-based metal-organic complexes (Fig. 3). A large amount of water molecules are located among the **CD-MONT-3** molecules and the solvent-accessible volume after the removal of uncoordinated solvents is 29.3%, which is slightly smaller than that of **CD-MONT-2**.

## Emission properties of CD-MONT-2 and CD-MONT-3

As we know, metal coordination significantly influences the photoluminescent properties in metal–organic complexes,<sup>22</sup> including MONTs (compared to organic ligands), which is an important property to be considered when trying to synthesize new photoluminescent materials. The emission spectra of **CD-MONT-2** and **CD-MONT-3** were measured at 77 K and 289 K, respectively, and they are displayed in Fig. 4. At 289 K, **CD-MONT-2** and **CD-MONT-3** exhibit photoluminescence at  $\lambda_{\text{max}} = 527$  and  $\lambda_{\text{max}} = 521$  nm (green region, Fig. 5), respectively, on excitation at 320 nm. As we know, cyclodextrins are non-aromatic ligands and photoluminescence silent. Emissions of cyclodextrins have been observed for other  $s^2$ -metal complexes and these emissions can be assigned to a metal-centered transition involving the  $s$  and  $p$  orbitals of  $\text{Pb(II)}$  ion, as proposed by Vogler *et al.*<sup>23</sup> Compared with the emission of **CD-MONT-2**, a 6-nm blue-shift is observed for **CD-MONT-3**, which may be the result of the existence of a larger lead cluster in **CD-MONT-3**. When cooling to 77 K, the emission band of **CD-MONT-2** blue-shifts 15 nm to 512 nm, accompanying a dramatic enhancement in intensity. Contrastingly, in the case of the **CD-MONT-3**, red-shifted photoluminescence at 531 nm with a slight enhancement is observed. The temperature-dependent photoluminescence behaviors may be attributed to the fact that the radiationless decay at lower temperatures could be reduced to some extent and then enhanced emissions were observed.<sup>24</sup>

## TGA and $\text{I}_2$ absorption behaviors of CD-MONT-2 and CD-MONT-3

TGA measurements for **CD-MONT-2** and **CD-MONT-3** show that both complexes lose uncoordinated solvents below 130 °C. It is known that CD molecules can encapsulate guests, such as pyrene, fullerene and halogen molecules *etc.*<sup>20,25</sup> In order to test the adsorption capacities of **CD-MONT-2** and **CD-MONT-3** to guest molecules, we used iodine molecules as the adsorbing target due to its easy estimation through colour change when adsorbed into a colourless crystal. **CD-MONT-2** and **CD-MONT-3** were heated to 120 °C for half an hour to release all of the solvents in

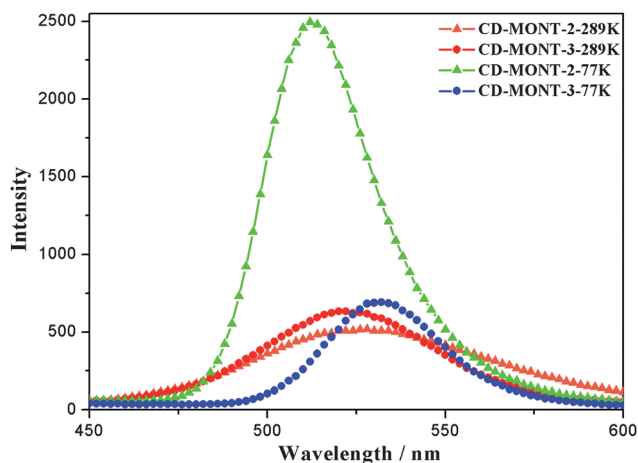


**Fig. 4** Solid-state emission spectra of **CD-MONT-2** and **CD-MONT-3** at 77 and 289 K.

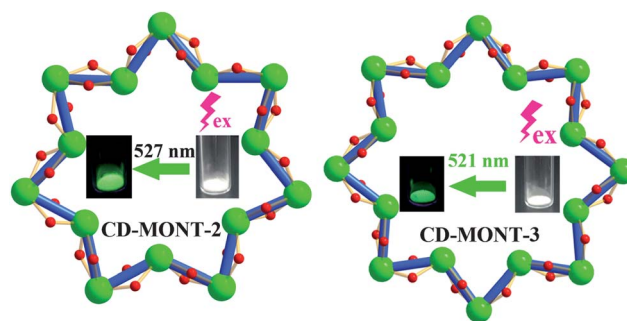


**Fig. 5** Photographs of the emissions from **CD-MONT-2** and **CD-MONT-3** in the solid state at room temperature under excitation of 365 nm.

the cavities to generate **CD-MONT-2'** and **CD-MONT-3'**. The XRPD patterns (Figs S10 and S11†) of the solvent-free **CD-MONT-2'** and **CD-MONT-3'** show no obvious change in comparison with the simulated patterns of **CD-MONT-2** and **CD-MONT-3**, indicating the maintenance of periodicity of the crystalline lattice upon extraction of lattice solvent molecules. After the activated samples were soaked in iodine solution (0.005 M) for 3 days, the colour of the solution changed from deep red to light pink (it was almost colourless for the **CD-MONT-2'** form) and the colour of the crystals also changed from their colourless state to brown and yellow for **CD-MONT-2'** and **CD-MONT-3'**, respectively (Fig. 6). These results indicate that iodine molecules were partly encapsulated in the cavities of **CD-MONT-2'** and **CD-MONT-3'**.<sup>26</sup> The adsorption capacity of **CD-MONT-2'** is much better than that of **CD-MONT-3'**, which can be estimated from the colour change of the toluene solution, as well as the crystals (Fig. 6). The reason for this can be fully explained by the difference in the 3D packing of **CD-MONT-2** and **CD-MONT-3**: **CD-MONT-2** contains large channels along the  $a$  axis, whereas **CD-MONT-3** is a nonporous supramolecule (Fig. 2(c, e)). An attempt to release iodine molecules from the cavities by soaking the samples in toluene failed, which indicates that **CD-MONT-2** and **CD-MONT-3** have high encapsulation capacity to iodine molecules and the adsorption is irreversible. The luminescence measurements reveal that emission intensities for the activated samples changed a lot for **CD-MONT-2'**, whereas they remained almost unchanged for **CD-MONT-3'**, as compared to the as-synthesized samples (Fig. S13†). These results indicate that the cyclohexanol solvents in the cavities have a significant effect on the emission of **CD-MONT-2**. However, emissions for the iodine-loaded samples changed dramatically and the intensity reduced significantly, which indicate that the adsorbed iodine molecules partly quenched the fluorescence of **CD-MONT-2** and **CD-MONT-3**.<sup>27</sup>

## DFT calculations

Attempts to obtain another member of this family, **CD-MONT-1** based on  $\alpha$ -CD, were unsuccessful. To explain the hard access of this mysterious member, we performed first principle calculations on the complex of  $\alpha$ -CD that cooperated with  $\text{Pb(II)}$  using the hybrid density functional theory method, in which the Beck three-parameter non-local exchange functional with the

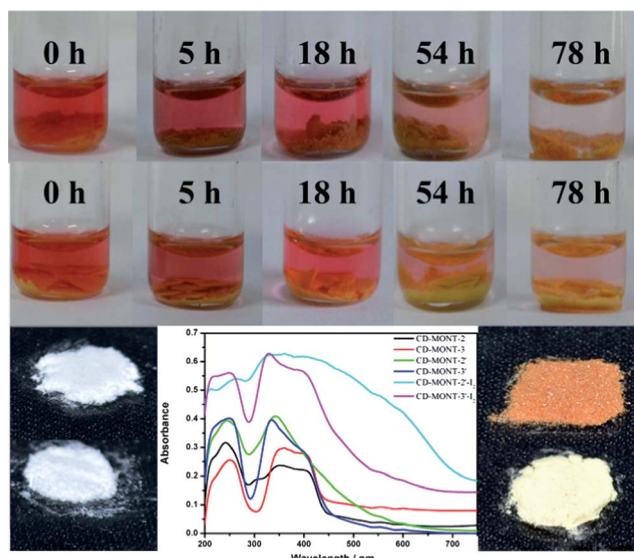


**Fig. 6** Photographs showing the visual colour change of iodine solution for **CD-MONT-2** (top) and **CD-MONT-3** (bottom) at 15 °C. In the photographs, the following are shown: crystals of **CD-MONT-2'** (left, top) and **CD-MONT-3'** (left, bottom) and their I<sub>2</sub>-loaded forms (right, top for **CD-MONT-2'-I<sub>2</sub>**; right, bottom for **CD-MONT-3'-I<sub>2</sub>**). The figure in the middle is the UV-Vis absorption spectra of the samples.

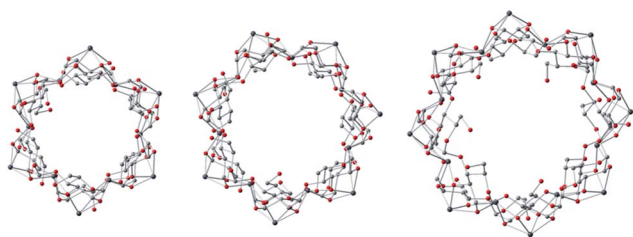


**Fig. 7** The optimized structures of **CD-MONT-1-3**.

correction functional of Lee–Yang–Parr (B3LYP) was used. The initial geometry of  $\alpha$ -CD was obtained from  $\beta$ -CD by cutting one pair of glucopyranose rings. **CD-MONT-1-3** based on  $\alpha, \beta, \gamma$ -cyclodextrins were fully optimized (Fig. 7). The calculation results (see Electronic Supporting Information†) suggest that **CD-MONT-1** has the largest dihedral angle of Pb–O–Pb–O in this family, giving the Pb ring in **CD-MONT-1** the largest torsion. Hence, the condition for construction of  $\alpha$ -CD-based MONT is harsh, and the assembly of  $\alpha$ -CD-based MONT is currently under way in our laboratory.

## Conclusions

In summary, two chiral Pb(II) discrete MONTs based on CD molecules were synthesized and characterized. We believe that a successful assembly of high yields of these nanotubular materials derives from the application of a biphasic solvothermal reaction. The functional MONTs emit green light under UV light at room temperature. Interestingly, the guest solvents in the cavity have a significant effect on the packing of the MONTs, resulting in the formation of porous and nonporous architectures for **CD-MONT-2** and **CD-MONT-3**, respectively. Both **CD-**

**MONT-2** and **CD-MONT-3** can encapsulate iodine molecules in the chiral cavities, which leads to the quenching of fluorescence. The present study highlights the significance of not only the synthesis strategy of tubular compounds but also guest solvents in the 3D packing of target compounds. Further studies will focus on the synthesis of d<sup>10</sup>- or 4f-metal complexes based on CD molecules by modifying the biphasic solvothermal reaction.

## Acknowledgements

This work was supported by the NSFC (Grant No. 90922014), the Shandong Natural Science Fund for Distinguished Young Scholars (2010JQE27021), the NSF of Shandong Province (BS2009L007, Y2008B01), Independent Innovation Foundation of Shandong University (2010JQ011 and 2011GN030) and the Special Fund for Postdoctoral Innovation Program of Shandong Province (201101007).

## References

- (a) S. Q. Ma, J. M. Simmons, D. Q. Yuan, J. R. Li, W. Weng, D. J. Liu and H.-C. Zhou, *Chem. Commun.*, 2009, 4049–4051; (b) L. Pan, D. H. Olson, L. R. Ciemnomolonski, R. Heddy and J. Li, *Angew. Chem., Int. Ed.*, 2006, **45**, 616–619; (c) G. Z. Yuan, C. F. Zhu, Y. Liu, W. M. Xuan and Y. Cui, *J. Am. Chem. Soc.*, 2009, **131**, 10452–10460; (d) J. N. Rebilly, J. Bacsá and M. J. Rosseinsky, *Chem.–Asian J.*, 2009, **4**, 892–903; (e) J. Zhang, S. M. Chen, T. Wu, P. Y. Feng and X. H. Bu, *J. Am. Chem. Soc.*, 2008, **130**, 12882–12883.
- (a) B. L. Chen, L. B. Wang, F. Zapata, G. D. Qian and E. B. Lobkovsky, *J. Am. Chem. Soc.*, 2008, **130**, 6718–6719; (b) V. Lykourinou, Y. Chen, X. S. Wang, L. Meng, T. Hoang, L. J. Ming, R. L. Musselman and S. Q. Ma, *J. Am. Chem. Soc.*, 2011, **133**, 10382–10385; (c) Q. L. Fang, G. S. Zhu, C. Jin, Y. Y. Ji, J. W. Ye, M. Xue, H. Yang, Y. Wang and S. L. Qiu, *Angew. Chem., Int. Ed.*, 2007, **46**, 6638–6642; (d) L. Han, M. C. Hong, R. H. Wang, J. H. Luo, Z. Z. Lin and D. Q. Yuan, *Chem. Commun.*, 2003, 2580–2581.
- (a) S. Tashiro, M. Tominaga, M. Kawano, M. T. Ozeki and M. Fujita, *J. Am. Chem. Soc.*, 2004, **126**, 10818–10819; (b) C. Y. Su, M. D. Smith and H. C. zur Loye, *Angew. Chem., Int. Ed.*, 2003, **42**, 4085–4089; (c) Z. Z. Lu, R. Zhang, Y. Z. Li, Z. J. Guo and H. G. Zheng, *J. Am. Chem. Soc.*, 2011, **133**, 4172–4174.
- (a) X. C. Huang, W. Luo, Y. F. Shen, X. J. Lin and D. Li, *Chem. Commun.*, 2008, 3995–3997; (b) H. F. Zhu, W. Zhao, T. Okamura, J. Fan, W. Y. Sun and N. Ueyama, *New J. Chem.*, 2004, **28**, 1010–1018; (c) S. L. Xiang, J. Huang, L. Li, J. Y. Zhang, L. Jiang, X. J. Kuang and C. Y. Su, *Inorg. Chem.*, 2011, **50**, 1743–1748.
- (a) P. Jensen, S. R. Batten, B. Moubaraki and K. S. Murray, *Chem. Commun.*, 2000, 793–794; (b) X. L. Wang, C. Qin, E. B. Wang, Y. G. Li, Z. M. Su, L. Xu and L. Carlucci, *Angew. Chem., Int. Ed.*, 2005, **44**, 5824–5827; (c) Y.-B. Dong, Y.-Y. Jiang, J. Li, J.-P. Ma, F.-L. Liu, B. Tang, R.-Q. Huang and S. R. Batten, *J. Am. Chem. Soc.*, 2007, **129**, 4520–4521.
- (a) T. T. Luo, H. C. Wu, Y. C. Jao, S. M. Huang, T. W. Tseng, Y. S. Wen, G. H. Lee, S. M. Peng and K. L. Lu, *Angew. Chem., Int. Ed.*, 2009, **48**, 9461–9464; (b) F.-N. Dai, H.-Y. He and D.-F. Sun, *J. Am. Chem. Soc.*, 2008, **130**, 14064–14065; (c) K. L. Huang, X. Liu, X. Chen and D. Q. Wang, *Cryst. Growth Des.*, 2009, **9**, 1646–1650.
- (a) G. Wenz, B. H. Han and A. Muller, *Chem. Rev.*, 2006, **106**, 782–817 and references therein; (b) Y. Liu, L. Yu, Y. Chen, Y. L. Zhao and H. Yang, *J. Am. Chem. Soc.*, 2007, **129**, 10656–10657; (c) Y. Liu, C. F. Ke, H. Y. Zhang, J. Cui and F. Ding, *J. Am. Chem. Soc.*, 2008, **130**, 600–605.
- (a) Y. Liu, S. H. Song, Y. Chen, Y. L. Zhao and Y. W. Yang, *Chem. Commun.*, 2005, 1702–1704; (b) Z. J. Ding, H. Y. Zhang, L. H. Wang, F. Ding and Y. Liu, *Org. Lett.*, 2011, **13**, 856–859; (c) A. Harada, R. Kobayashi, Y. Takashima, A. Hashidzume and H. Yamaguchi, *Nat. Chem.*, 2011, **3**, 34–37.

- 9 E. Lee, J. Heo and K. Kim, *Angew. Chem., Int. Ed.*, 2000, **39**, 2699–2701.
- 10 (a) R. A. Smaldone, R. S. Forgan, H. Furukawa, J. J. Gassensmith, A. M. Z. Slawin, O. M. Yaghi and J. F. Stoddart, *Angew. Chem., Int. Ed.*, 2010, **49**, 8630–8634; (b) J. J. Gassensmith, H. Furukawa, R. A. Smaldone, R. S. Forgan, O. M. Yaghi and J. F. Stoddart, *J. Am. Chem. Soc.*, 2011, **133**, 15312–15315; (c) R. S. Forgan, R. A. Smaldone, J. J. Gassensmith, H. Furukawa, D. B. Cordes, Q. Li, C. E. Wilmer, R. Q. Snurr, A. M. Z. Slawin and J. F. Stoddart, *J. Am. Chem. Soc.*, 2012, **134**, 406–417.
- 11 P. Klufers and J. Schuhmacher, *Angew. Chem., Int. Ed.*, 1994, **33**, 1863–1865.
- 12 (a) P. M. Forster and A. K. Cheetham, *Angew. Chem., Int. Ed.*, 2002, **41**, 457–459; (b) T. P. Hu, H. Y. He, F. N. Dai, X. L. Zhao and D. F. Sun, *CrystEngComm*, 2010, **12**, 2018–2020.
- 13 Bruker. *SMART, Saint and SADABS*. Bruker AXS Inc., Madison, Wisconsin, USA, 1998.
- 14 (a) G. M. Sheldrick, *SHELXS-97, Program for X-ray Crystal Structure Determination*, University of Göttingen, Germany, 1997; (b) G. M. Sheldrick, *SHELXL-97, Program for X-ray Crystal Structure Refinement*, University of Göttingen, Germany, 1997.
- 15 R. G. Satink, G. Meijer and G. V. Helden, *J. Am. Chem. Soc.*, 2003, **125**, 15714–15715.
- 16 (a) M. Affronte, S. Carretta, G. A. Timco and R. E. P. Winpenny, *Chem. Commun.*, 2007, 1789–1797; (b) C. Y. Su, X. P. Yang, B. S. Kang and T. C. W. Mak, *Angew. Chem., Int. Ed.*, 2001, **40**, 1725–1728; (c) M. Oh, X. F. Liu, M. Park, D. Kim, D. Moon and M. S. Lah, *Dalton Trans.*, 2011, **40**, 5720–5727; (d) G. L. Wang, Y. J. Lin and G. X. Jin, *Chem.–Eur. J.*, 2011, **17**, 5578–5587; (e) L. Y. Yao, L. Qin, T. Z. Xie, Y. Z. Li and S. Y. Yu, *Inorg. Chem.*, 2011, **50**, 6055–6062; (f) G. Swiegers and T. J. Malefetse, *Chem. Rev.*, 2000, **100**, 3483–3538; (g) P. Thuery, C. Villiers, J. Jaud, M. Ephritikhine and B. Masci, *J. Am. Chem. Soc.*, 2004, **126**, 6838–6839; (h) E. Coronado, J. R. Galan-Mascaros, P. Gavina, C. Marti-Gastaldo, F. M. Romero and S. Tatay, *Inorg. Chem.*, 2008, **47**, 5197–5203; (i) C. M. Jin, H. Lu, L. Y. Wu and J. Huang, *Chem. Commun.*, 2006, 5039–5041.
- 17 P. D. Beer, M. G. B. Drew, P. A. Gale, M. I. Ogden and H. R. Powell, *CrystEngComm*, 2000, **2**, 164–168.
- 18 (a) C. F. Lee, D. A. Leigh, R. G. Pritchard, D. Schultz, S. J. Teat, G. A. Timco and R. E. P. Winpenny, *Nature*, 2009, **458**, 314–318; (b) H. N. Miras, I. Chakraborty and R. G. Raptis, *Chem. Commun.*, 2010, **46**, 2569–2571; (c) Y. F. Bi, G. C. Xu, W. P. Liao, S. C. Du, X. W. Wang, R. P. Deng, H. J. Zhang and S. Gao, *Chem. Commun.*, 2010, **46**, 6362–6364; (d) W. L. Liu, K. Lee, M. Park, R. P. John, D. Moon, Y. Zou, X. F. Liu, H. Ri, G. H. Kim and M. S. Lah, *Inorg. Chem.*, 2008, **47**(19), 8807–8812; (e) H. X. Li, H. Z. Wu, W. H. Zhang, Z. G. Ren, Y. Zhang and J. P. Lang, *Chem. Commun.*, 2007, 5052–5054; (f) O. L. Sydora, P. T. Wolczanski, E. B. Lobkovsky, E. Rumberger and D. N. Hendrickson, *Chem. Commun.*, 2004, 650–651; (g) J. Y. Hu, J. A. Zhao, Q. Q. Guo, H. W. Hou and Y. T. Fan, *Inorg. Chem.*, 2010, **49**, 3679–3681; (h) D. Puerta and S. M. Cohen, *Chem. Commun.*, 2003, 1278–1279.
- 19 R. P. John, M. Park, D. Moon, K. Lee, S. Hong, Y. Zou, C. S. Hong and M. S. Lah, *J. Am. Chem. Soc.*, 2007, **129**, 14142–14143.
- 20 (a) T. Kida, T. Lwamoto, Y. Fujino, N. Tohnai, M. Miyata and M. Akashi, *Org. Lett.*, 2011, **13**, 4570–4573; (b) X. Cheng, Z. D. Lu, Y. Z. Li, Q. Wang, C. S. Lu and Q. J. Meng, *Dalton Trans.*, 2011, **40**, 11788–11794.
- 21 A. L. Spek, *J. Appl. Crystallogr.*, 2003, **36**, 7–13.
- 22 S. Deo and H. A. Godwin, *J. Am. Chem. Soc.*, 2000, **122**, 174–175.
- 23 P. C. Ford and A. Vogler, *Acc. Chem. Res.*, 1993, **26**, 220–226.
- 24 Q. Zhu, C. Shen, C. Tan, T. Sheng, S. Hu and X. Wu, *Chem. Commun.*, 2012, **48**, 531–533.
- 25 (a) K. A. Connors, *Chem. Rev.*, 1997, **97**, 1325–1358; (b) A. Ikeda, R. Aono, N. Maekubo, S. Katao, J. Kikuchi and M. Akiyama, *Chem. Commun.*, 2011, **47**, 12795–12797.
- 26 M. H. Zeng, Q. X. Wang, Y. X. Tan, S. Hu, H. X. Zhao, L. S. Long and M. Kurmoo, *J. Am. Chem. Soc.*, 2010, **132**, 2561–2563.
- 27 (a) S. M. Singleton and R. D. Coombe, *J. Phys. Chem.*, 1995, **99**, 16296–16300; (b) Q. K. Liu, J. P. Ma and Y. B. Dong, *Chem. Commun.*, 2011, **47**, 7185–7187; (c) J. R. Lakowicz, *Principles of fluorescence spectroscopy*, Springer, 3rd edn, 2006.